



Microstructure evolution of directionally solidified DZ125 superalloy with melt superheating treatment

Changshuai Wang, Jun Zhang*, Lin Liu, Hengzhi Fu

State Key Laboratory of Solidification Processing, Northwestern Polytechnical University, Xi'an 710072, Shaanxi, China

ARTICLE INFO

Article history:

Received 13 April 2010

Received in revised form 15 August 2010

Accepted 24 August 2010

Available online 28 September 2010

Keywords:

High-temperature alloys

Crystal growth

Microstructure

Scanning electron microscopy

ABSTRACT

The melt superheating treatment is carried out for DZ125 superalloy during directional solidification. Under the same thermal gradient and solidification velocity, the microstructure evolution of directionally solidified DZ125 superalloy is systematically investigated by changing the melt superheating temperature. The results show that the dendrite is refined with the melt superheating temperature increasing from 1500 °C to 1650 °C. However, it becomes coarse after the melt superheating treatment at 1750 °C. The dendrite segregation first reduces with the increase of melt superheating temperature between 1500 °C and 1650 °C, but becomes more severe when the superheating temperature is higher than 1650 °C. The carbide morphology presents script-like when the melt superheating temperature is below 1600 °C. Further increasing the melt superheating temperature, it is mainly blocky and nodular. Moreover, the reason of microstructure evolution with melt superheating treatment is discussed. The results are useful for promoting the development of high quality directionally solidified superalloy.

© 2010 Elsevier B.V. All rights reserved.

1. Introduction

As a precipitation hardened directionally solidified Ni-base superalloy, DZ125 has been widely applied as structural materials in advanced aeroengine for gas turbine blades and vanes operating at high temperature. The high temperature capabilities of superalloys are decided by the solidification microstructure on a large scale. In order to improve the solidification structure, many studies have been done in many aspects [1–7], especially in solidification processing and alloy composition. The addition of refractory elements allows remarkable improvement in high temperature creep resistance [6]. However, this gives rise to a large-scale increase of the production cost and the appearance of topologically close-packed phases. The high thermal gradient directional solidification can achieve finer dendrite arm, reduce element segregation and increase stress rupture life [1,3], but it is limited [8].

Recently, it has been found that under the same solidification condition, the melt structure has obvious influence on solidification microstructure and mechanical property of alloy [9–11]. The structure of alloy melt is not only related with the composition and temperature but also with the thermal history of melt [12–14]. It has been shown that the melt structure, the solidification microstructure and the performance of Al–Si alloy, Mg–Si

alloy and Ti–Al alloy can be significantly modified by the melt superheating treatment [11,15]. It was also found that the wettability of Sn–0.7Cu alloy was improved after melt superheating treatment [10]. However, until now, the researches mainly focus on simple alloys. For Ni-base superalloy, most attention has been paid on traditional casting superalloy [16] and single crystal superalloy [17–19] grown by different methods, such as gradient method, Bridgman technique with spontaneous nucleation and with seed [20], and Czochralski method [21]. Yin et al. [16] have found that the grain is refined after melt superheating treatment. For DD3 single crystal superalloy, the melt superheating treatment can refine dendrite arm, reduce element segregation and improve stress rupture property [19]. Directional solidification superalloy is important commercial alloy. Nevertheless, hitherto, there are few researches about the influence of melt superheating treatment on the microstructure of directionally solidified Ni-base superalloy with complex phase. Therefore, a systematic research is needed to study the relationship between melt superheating treatment and solidification microstructure of directionally solidified Ni-base superalloy with complex phase.

In this paper, under constant thermal gradient and solidification velocity, the melt superheating treatment during directional solidification is carried out for DZ125 directionally solidified Ni-based superalloy by changing the melt superheating temperature. The purpose is to study the influence of melt superheating treatment on microstructure and microsegregation of DZ125 directionally solidified Ni-based superalloy and to develop a new casting process route to refine microstructure and reduce segregation.

* Corresponding author. Tel.: +86 29 8849 4825; fax: +86 29 8849 4825.
E-mail address: zhjscott@nwpu.edu.cn (J. Zhang).

Table 1

The chemical composition of DZ125 superalloy (wt.%).

Superheating temperature (°C)	Alloy composition							
	Cr	Co	W	Mo	Al	Ti	Ta	Ni
1500	8.59	9.48	6.87	2.50	5.37	1.19	4.19	Bal.
1600	8.60	9.42	6.75	2.51	5.42	1.20	4.18	
1650	8.59	9.47	6.68	2.46	5.50	1.16	4.16	
1750	8.55	9.52	6.72	2.51	5.46	1.20	4.28	

2. Experimental

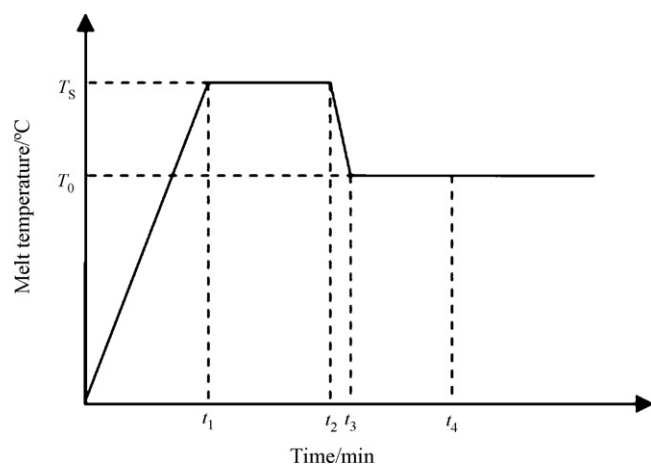
The chemical composition of the experimental superalloy DZ125, as measured by using a SPECTRO MAXx Direct-reading Spectrograph (DIA2000SE), is shown in Table 1. Cylindrical bars of DZ125 with 7.0 mm diameter and 80 mm length were prepared by liquid metal cooling directional solidification technique under high purity argon atmosphere. During the melt superheating treatment process (see Fig. 1), the sample was first superheated to melt superheating temperature T_s . After kept at T_s for a period of time (t_s), the sample was rapidly cooled down to T_0 and then held at T_0 for another space (t_h) to guarantee the uniform of melt temperature and the same thermal gradient for all experiments. Finally, it was withdrawn into the Ga–In–Sn liquid metal bath to complete the crystal growth. In the present paper, four T_s , i.e. 1500 °C, 1600 °C, 1650 °C, 1750 °C were selected. The T_0 was 1500 °C. The held periods at T_s and T_0 were $t_s = (t_2 - t_1) = 30$ min and $t_h = (t_4 - t_3) = 30$ min, respectively. After 30 min at T_0 to keep the thermal gradient unchanged, all samples were withdrawn into the liquid Ga–In–Sn alloy at the same rate of $R = 50$ $\mu\text{m/s}$. Because T_0 and R were the same for all different T_s , the thermal gradient G will remain invariable for all experiments.

The microstructure was observed by Leica DM-4000M microscope and TESCAN VEGA\\LMH scanning electron microscope. The microsegregation was measured by JXA-8100 electron probe microscope. The primary dendrite arm spacing was measured over the central region of the solidified samples, where the steady-state growth conditions were achieved. Primary dendrite arm spacing (λ_1) was estimated from transverse section using the relationship $\lambda_1 = (A/n)^{0.5}$ (where n is the number of primary dendrite in a known area A). Secondary dendrite arm spacing was measured from longitudinal sections and well-aligned dendrite trunks. Secondary dendrite arm spacing (λ_2) was calculated by using $\lambda_2 = L/N_2$, where L was the length of well-aligned dendritic trunks (from the middle part of the first to the $N_2 + 1$ secondary dendrite arm) and N_2 was the number of secondary dendrite arms along the segment L . The segregation ratio of every element was determined as the extreme concentration in interval area over that in crystallizing core [22].

3. Results

3.1. Dendrite arm spacing

The morphology of primary dendrite for different melt superheating temperatures is shown in Fig. 2. It can be clearly seen that the primary dendrite arms are continuously refined with the increase of melt superheating temperature when it is less than 1650 °C. However, further increasing the melt superheating temperature, the primary dendrite arms become coarse. For the

**Fig. 1.** Melt superheating treatment regulation.

selected four melt superheating temperatures 1500 °C, 1600 °C, 1650 °C and 1750 °C, the corresponding primary dendrite arm spacings measured are 141.4 ± 3 μm , 132.9 ± 2 μm , 125.0 ± 1 μm and 147.3 ± 4 μm , respectively. The maximum reduction rate of λ_1 is 11.6%. Fig. 3 shows the morphology evolution of secondary dendrite for different melt superheating temperatures. Obviously, the variation of secondary dendrite arms is similar to that of the primary dendrite arm, i.e. the second dendrite arm spacings first decrease until to 1650 °C and then increase. Meanwhile, the second dendrite arm spacings measured are 33.1 ± 1.5 μm , 29.0 ± 1 μm , 25.1 ± 1 μm and 30.5 ± 1.3 μm , respectively. The maximum reduction rate of λ_2 is about 18.3%. On this basis, Fig. 4 presents the plot of primary dendrite arm spacing and second dendrite arm spacing as a function of melt superheating temperature. This is different from the results of single crystal superalloy DD3. The dendrite arm spacing of DD3 is continuously refined with the increase of melt superheating temperature [19].

3.2. Dendrite segregation ratios

Fig. 5 illustrates the variation of element segregation ratios with the increase of melt superheating temperature. It can be clearly seen that the segregation ratios of Mo, Ti and Ta are all larger than 1, while those of Co and W are smaller than 1, and that for Al and Cr are very close to 1. Meanwhile, it can be inferred that the melt superheating treatment reduces the segregation of Mo, W, Ta and Ti, but has no obvious influence on the dendrite segregation ratios of Al, Cr and Co when the melt superheating temperature is below 1650 °C. But, the segregation becomes severe when the melt superheating temperature is 1750 °C.

3.3. Carbide morphology

The typical carbide morphology (white zone) of the directionally solidified superalloy is shown in Fig. 6. In the case of 1500 °C, which means no melt superheating treatment, the morphology of the MC carbide phase is script-like (Fig. 6(a)). When the melt is superheated to 1600 °C, the morphology of carbide phase has no obvious variation, except for the decrease of the size of MC carbide (Fig. 6(b)). As the melt is superheated to 1650 °C, the morphology of MC carbide mainly presents blocky and nodular (Fig. 6(c)). When the melt is further superheated to 1750 °C, the morphology of MC carbide is still mainly blocky and nodular, but the amount of carbide decreases (Fig. 6(d)).

4. Discussion

The above experimental results indicate that suitable melt superheating treatment can refine dendrite structure, reduce dendrite segregation and improve carbide morphology. From Table 1, it can be seen that the melt superheating treatment has no influence on composition of DZ125 when the melt superheating temperature is less than 1750 °C. In addition, all the experiments are processed at the same thermal gradient and solidification velocity after melt superheating treatment. Therefore, the variation of solidification microstructure for the elevated superheating temperature cannot

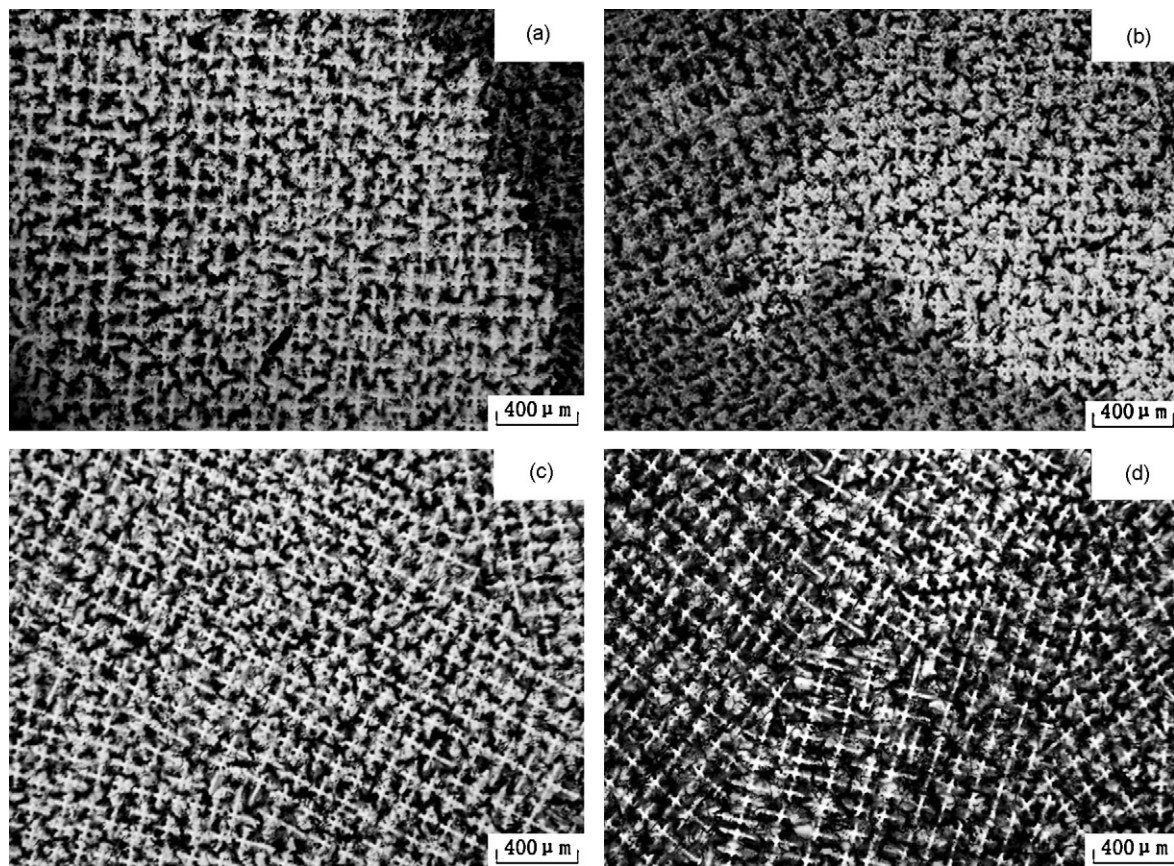


Fig. 2. Primary dendrite morphology for different melt superheating temperatures (a) $T_s = T_0 = 1500^\circ\text{C}$; (b) $T_s = 1600^\circ\text{C}$; (c) $T_s = 1650^\circ\text{C}$ and (d) $T_s = 1750^\circ\text{C}$.

be owing to the external solidification parameters and alloy composition, but should be attributed to the change of internal melt structure.

The alloy melt consists of clusters which have the structure similar to that of solid phase when the melt temperature is a little higher than the liquidus. These clusters are very stable even though they are not in thermodynamic equilibrium. Popel et al. [23] discovered that the melt structure transformed from a microinhomogeneous to a homogeneous state when the melt superheating temperature passed critical temperature. For Ni-base superalloy, which contains carbide, there are two critical temperatures. The superalloy melt consists of interacting Ni_3 (Al, Ti)-like cluster, residual MC carbide and other high-melting particle when the melt temperature is a little higher than the liquidus [16,24]. When the melt temperature reaches the first critical temperature (t_{aH1}), the melt structure is complex cluster of high-melting-point particle surrounded by Ni_3 (Al, Ti)-like cluster. The complex cluster is destroyed, the structure and the composition of melt become more homogeneous, when the melt temperature is higher than second critical temperature (t_{aH2}) [25].

The equilibrium of melt structure needs a relaxation time which is much longer than the thermal equilibrium relaxation time [26]. As a result, the melt structure partly remains its high temperature structure when it is quickly cooled from T_s to T_0 . Consequently, after melt superheating treatment, the composition, distribution and the structure of clusters in the melt are different from that without melt superheating treatment even if the temperature of alloy melt is decreased from T_s to T_0 .

It is evident that the change of alloy melt structure will influence the solidification process [27]. Kolotukhin and Tjagunov [25] studied the influence of melt superheating temperature on solidification process of superalloy with various contents of carbon. It

was found that the freezing range decreased with the increase of T_s when T_s was less than t_{aH2} . However, further increasing the T_s , the freezing range became large. The non-linear variation of freezing range is related to the difference of the disappearing critical temperature of Ni_3 (Al, Ti, Nb)-like cluster and MC carbide or (Ti, Nb) C cluster [25]. Zu et al. [28] also found that the undercooling degree of nucleation increased and solidification time reduced with increasing the melt superheating temperature. It is well known that the freezing range is one of the factors that influence the dendrite arm spacing. Therefore, under the same thermal gradient and solidification velocity, one possible explanation is that the variation of freezing range leads to the change of dendrite arm spacing. The difference of dendrite arm spacing change between DD3 and DZ125 should be attributed to the difference of alloy composition. The t_{aH2} increases with the decrease of carbon concentration [25]. The carbon concentration of DD3 is less than DZ125. That is to say that the t_{aH2} of DD3 is higher than DZ125. Therefore, the dendrite arm spacing of DD3 can be continuously refined even if the melt superheating temperature is up to 1780°C .

The value of solute distribution coefficient of alloy element, k , is closely related to its activity coefficient, which is the function of the interaction among atoms and clusters in alloy melt. So the variation of the interaction among atoms and clusters in alloy melt will affect the solute distribution coefficient. The melt structure of alloy is related with the thermal history of the sample. After melt superheated treatment, the composition, distribution and the structure of clusters in the melt are different from that without melt superheating treatment even if the temperature of alloy melt is decreased from T_s to T_0 . This leads to the change of interaction among clusters and atoms in alloy melt. Consequently, the solute distribution coefficient of the alloy elements after the melt superheating treatment is different from that without melt super-

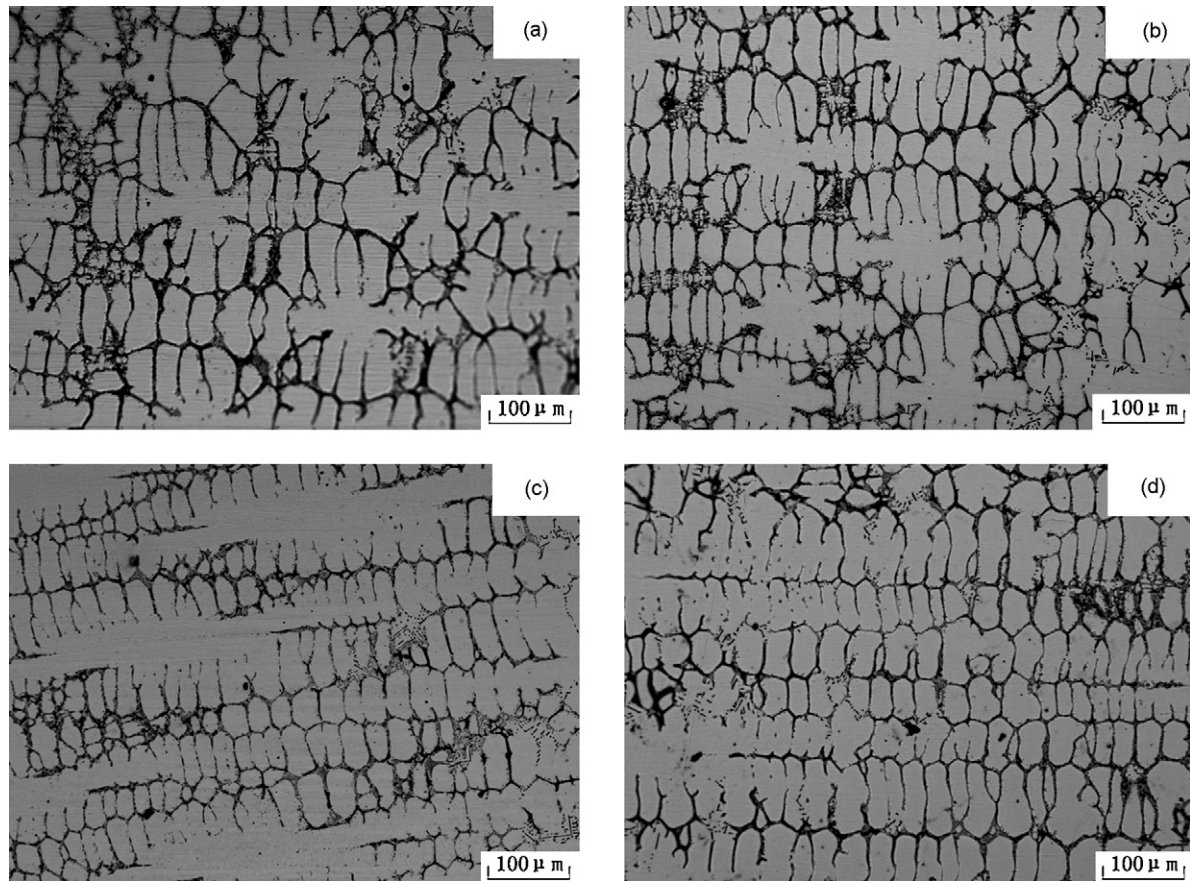


Fig. 3. Secondary dendrite morphology under different melt superheating temperatures (a) $T_s = T_0 = 1500^\circ\text{C}$; (b) $T_s = 1600^\circ\text{C}$; (c) $T_s = 1650^\circ\text{C}$ and (d) $T_s = 1750^\circ\text{C}$.

heating treatment. The segregation situation is related with the solute distribution coefficient. Therefore, the segregation situation is obviously changed after melt superheating treatment. The non-linear variation of segregation situation is possibly related to the difference of the disappearing temperature of Ni_3 (Al, Ti, Nb)-like cluster and MC carbide or (Ti, Nb) C cluster.

Generally speaking, the crystal growth from the melt needs sufficient solute supersaturation, enough growth space and time. For the dendritic structure at lower value of G/R , the residual melt exists in the interdendritic region, creating a favourable condition for the

growth of carbide branches and resulting in script type morphology [29]. If the alloy melt is superheated above critical temperature, the MC carbide will be dissolved and the distribution of alloy elements will tend to be more homogeneous [16,30], which will make the nucleation and growth of carbide difficult. Therefore, the formation of carbide is postponed. The growth space and time are decreased. The reduction of microsegregation decreases the content of formation elements of carbide in the interdendrite area. They are unfavourable conditions for the growth of carbide. There-

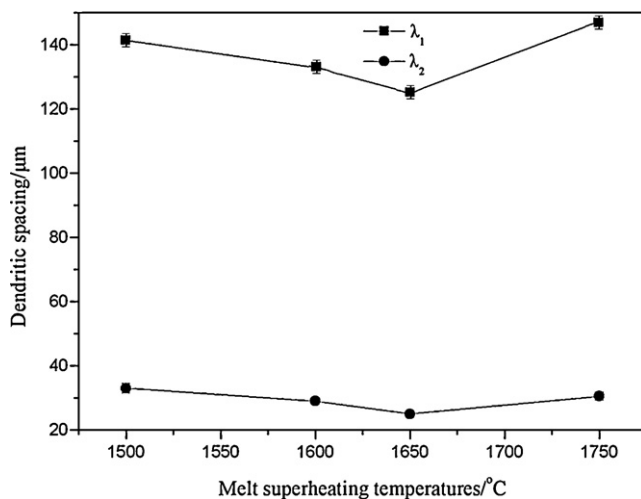


Fig. 4. Primary and secondary arm spacing as a function of melt superheating temperature.

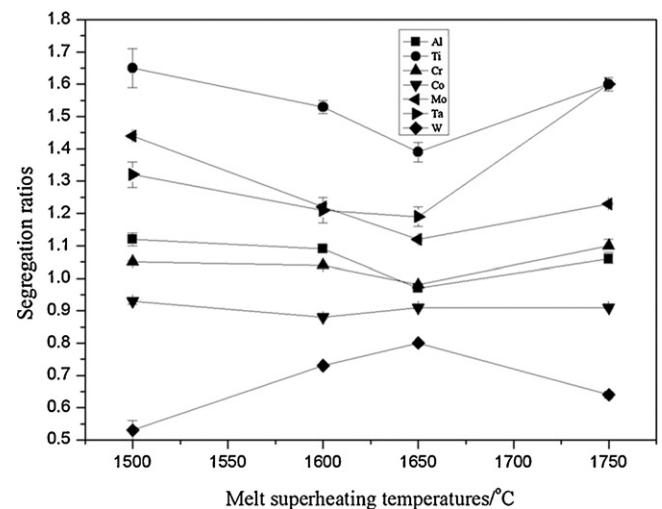


Fig. 5. Relationship between dendrite segregation ratios and melt superheating temperature.

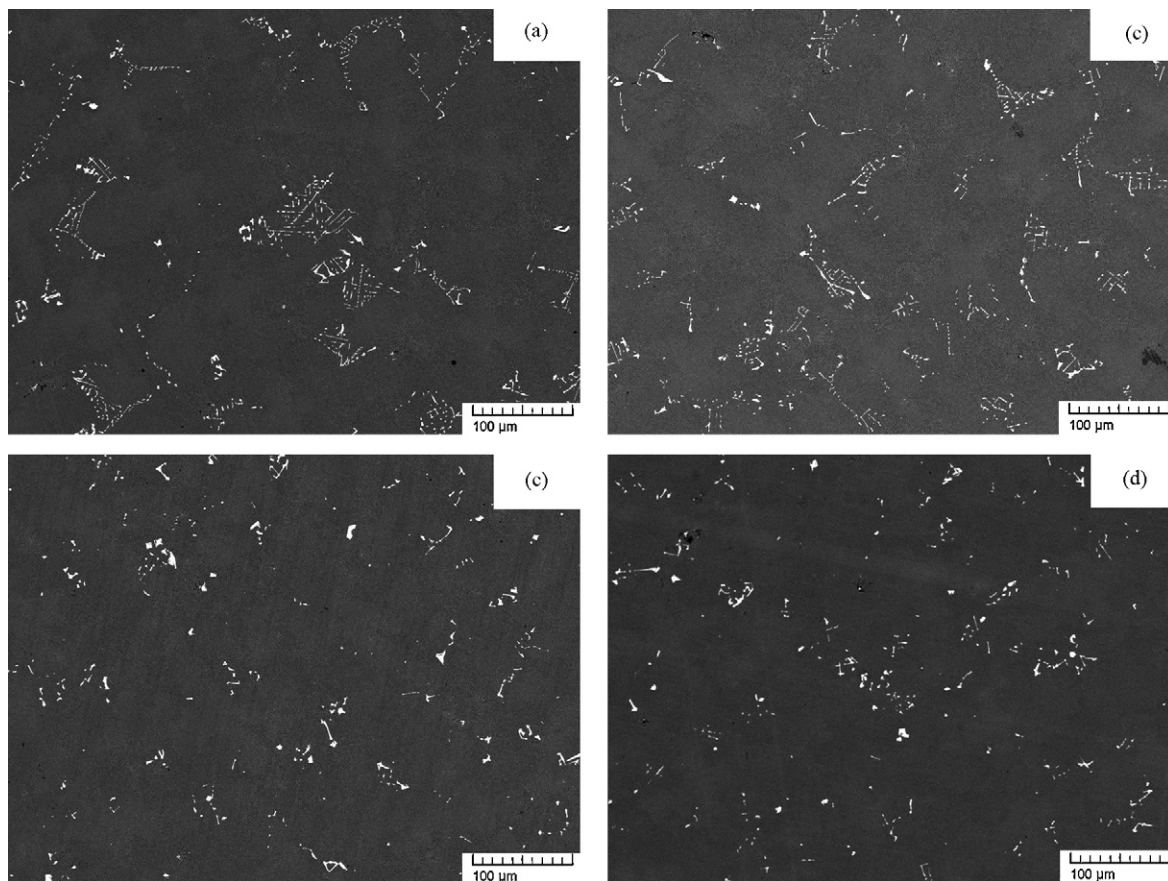


Fig. 6. Carbide morphology of DZ125 superalloy for different melt superheating temperatures (a) $T_s = T_0 = 1500\text{ }^{\circ}\text{C}$; (b) $T_s = 1600\text{ }^{\circ}\text{C}$; (c) $T_s = 1650\text{ }^{\circ}\text{C}$ and (d) $T_s = 1750\text{ }^{\circ}\text{C}$.

fore the morphology of carbide presents from script-like to blocky and nodular. That is to say the reason for the variation of carbide morphology is the change of the carbide growth condition when the melt superheat temperature increases from $1500\text{ }^{\circ}\text{C}$ to $1750\text{ }^{\circ}\text{C}$.

Therefore, the reasons for the change of dendrite arm spacing, alloy element segregation ratios and carbide morphology may be attributed to the variation of melt structure. The variation of dendrite arm spacing and alloy element segregation ratios is resulted from the change of freezing range and solute distribution coefficient. The change of MC carbide morphology and size are related to the disappearance of MC carbide clusters in melt and the reduction of alloy element segregation after melt superheating treatment.

5. Conclusions

The effect of melt superheating treatment on microstructure of DZ125 superalloy during directional solidification has been investigated. The results indicate that the dendrite is refined and segregation is reduced with the melt superheating temperature increasing from $1500\text{ }^{\circ}\text{C}$ to $1650\text{ }^{\circ}\text{C}$. Further superheated to $1750\text{ }^{\circ}\text{C}$, the dendrite is coarse and segregation situation becomes serious. With the increase of the melt superheating temperature, the morphology of MC carbide changes from scrip-like to blocky and nodular.

Acknowledgements

The authors would gratefully acknowledge the financial support from National Nature Science Foundation of China (Grant No. 50931004), National Basic Research Program of China (Grant No. 2006CB605202 and Grant No. 2010CB631202) and National

High Technology Research and Development Program (Grant No. 2007AA03Z552).

References

- [1] L. Liu, T.W. Huang, J. Zhang, H.Z. Fu, *Mater. Lett.* 61 (2007) 227–230.
- [2] B.C. Wilson, E.R. Cutler, G.E. Fuchs, *Mater. Sci. Eng. A* 479 (2008) 356–364.
- [3] K. Zhao, Y.H. Ma, L.H. Lou, *J. Alloys Compd.* 475 (2009) 648–651.
- [4] H. Lefaix, P. Vermaut, D. Janickovic, P. Svec, R. Portier, F. Prima, *J. Alloys Compd.* 483 (2009) 168–172.
- [5] M. Asta, C. Beckermann, A. Karma, W. Kurz, R. Napolitano, M. Plapp, G. Purdy, M. Rappaz, R. Trivedi, *Acta Mater.* 57 (2009) 941–971.
- [6] J. Zhang, J.G. Li, T. Jin, X.F. Sun, Z.Q. Hu, *Mater. Sci. Eng. A* 527 (2010) 3051–3056.
- [7] X.F. Ding, J.P. Lin, L.Q. Zhang, H.L. Wang, G.J. Hao, G.L. Chen, *J. Alloys Compd.* (2010), doi:10.1016/j.jallcom.2010.06.151.
- [8] L. Liu, T.W. Huang, M. Qu, G. Liu, J. Zhang, H.Z. Fu, *J. Mater. Process. Technol.* 210 (2010) 159–165.
- [9] Z.H. Gu, H.Y. Wang, N. Zheng, M. Zha, L.L. Jiang, W. Wang, Q.C. Jiang, *J. Mater. Sci.* 43 (2008) 980–984.
- [10] X.F. Li, F. Zhang, F.Q. Zu, X. Lv, Z.X. Zhao, D.D. Yang, *J. Alloys Compd.* (2010), doi:10.1016/j.jallcom.2010.06.087.
- [11] D. Qiu, M.X. Zhang, J.A. Taylor, H.M. Fu, P.M. Kelly, *Acta Mater.* 55 (2007) 1863–1871.
- [12] P.S. Popel, V.E. Sidorov, *Mater. Sci. Eng. A* 226–228 (1997) 237–244.
- [13] V. Sidorov, P. Popel, L. Son, L. Malyshev, *Mater. Sci. Eng. A* 226–228 (2001) 317–320.
- [14] F.S. Yin, X.F. Sun, H.R. Guan, Z.Q. Hu, *J. Alloys Compd.* 364 (2004) 225–228.
- [15] K. Jiang, X.F. Liu, *J. Alloys Compd.* 484 (2009) 95–101.
- [16] F.S. Yin, X.F. Sun, J.G. Li, H.R. Guan, Z.Q. Hu, *Scripta Mater.* 48 (2003) 425–429.
- [17] L. Liu, T.W. Hang, M.M. Zou, W.G. Zhang, J. Zhang, H.Z. Fu, *Proceedings of the 11th International Symposium Superalloys 2008, Pennsylvania, USA, 2008*, pp. 287–293.
- [18] M.M. Zou, J. Zhang, B. Li, L. Liu, H.Z. Fu, *Int. J. Mod. Phys. B* 23 (2009) 1105–1109.
- [19] J. Zhang, B. Li, M.M. Zou, C.S. Wang, L. Liu, H.Z. Fu, *J. Alloys Compd.* 484 (2009) 753–756.
- [20] S. Kostic, A. Golubovic, A. Valcic, *J. Serb. Chem. Soc.* 74 (2009) 61–69.
- [21] W.M. Li, S. Kou, *J. Cryst. Growth* 177 (1997) 140–144.
- [22] X.P. Guo, H.Z. Fu, J.H. Sun, *Metall. Trans. A* 28 (1997) 997–1009.

- [23] P.S. Popel, M. Calvo-Dahlborg, U. Dahlborg, J. Non-cryst. Solids 353 (2007) 3243–3253.
- [24] F.S. Yin, Q. Zheng, X.F. Sun, H.R. Guan, Z.Q. Hu, J. Mater. Process. Technol. 183 (2007) 440–444.
- [25] E.V. Kolotukhin, G.V. Tjagunov, J. Mater. Process. Technol. 53 (1995) 219–227.
- [26] G. Chen, J.W. Yu, H.Z. Fu, J. Mater. Sci. Lett. 18 (1999) 1571–1573.
- [27] H. Fredriksson, E. Fredriksson, Mater. Sci. Eng. A 413–414 (2005) 455–459.
- [28] F.Q. Zu, G.H. Ding, X.F. Li, J. Cryst. Growth 310 (2008) 397–403.
- [29] L. Liu, F. Sommer, H.Z. Fu, Scripta Mater. 30 (1994) 587–591.
- [30] L. Liu, B.L. Zhen, A. Banerji, W. Reif, F. Sommer, Scripta Mater. 30 (1994) 593–598.